Dielectric response of multiwalled carbon nanotubes as a function of applied ac-electric fields

Rajratan Basu and Germano S. Iannacchione[a)]
Department of Physics, Order-Disorder Phenomena Laboratory, Worcester Polytechnic Institute, Worcester, Massachusetts 01609, USA

(Received 18 July 2008; accepted 19 October 2008; published online 5 December 2008)

The complex dielectric constant (ε^*) is reported for multiwalled carbon nanotubes (MWCNTs) up to 10^5 Hz as a function of ac-electric field amplitudes E_{rot} (in phase and same frequency as the measurement) and E_{ac} (different phase and fixed frequency with respect to the measurement). A slow relaxation process (mode 1) is observed, which shifts to higher frequency with increasing E_{rot} but is independent of E_{ac}. A fast relaxation process (mode 2) is also observed, which is independent of E_{rot} but shifts to higher frequency with increasing E_{ac} (opposite to that of mode 1). An ac-conductivity analysis of MWCNT reveals insights on how E_{rot} and E_{ac} influence the dissipation.
 [DOI: 10.1063/1.3035963]

I. INTRODUCTION

One-dimensional carbon nanotubes (CNTs) have been of intense research interest due to their unique atomic and electronic structures (Ref. 1). In addition to their extraordinary thermal, mechanical, and magnetic properties,[2–12] their unique electrical character makes them potentially useful materials for use in nanoelectronic devices.[13–17] The dielectric storage and loss properties are of special interest to researchers and engineers as these two parameters, among others, provide insight to CNTs and their suitability for electronic applications.

In recent years, a CNT dispersion in an anisotropic liquid media (such as a liquid crystal) has gained interest for inducing parallel alignment of CNTs and ac-field induced orientation manipulation for use as switches at the nanoscale level.[18–20] In these kinds of applications, it is important to know the dynamic dielectric modes of CNTs as well as their behavior under an applied ac-electric field. Dielectric spectroscopy of CNTs can reveal insights on those dynamic modes of potential interests as a function of ac field intensity.

Aggregated CNTs show unique dielectric spectra,[21] and the relaxation mechanisms are found to be distorted upon application of electric fields. However, the experimental application of an external ac-electric field can be complicated. For example, the probing field $E_{rot}(\omega)$ in an ac-capacitive measurement is in phase and at the same frequency ω as the measurement of the complex dielectric constant $\varepsilon^*(\omega)=\varepsilon' - i\varepsilon''$. Thus, in the complex *rotating frame* of the measurement, E_{rot} can be considered a "static" field. Conversely, the applied ac-electric field may be at a fixed frequency ω' with respect to the ac-capacitive measurement frequency ω, i.e., $\omega'=\text{const}>\omega$. The field $E_{ac}(\omega')$ is an oscillating field in the complex rotating frame of the measurement. Figure 1 illustrates the phasor diagram of these two electric fields.

In this paper, the focus is to understand the dielectric response of CNTs with respect to applied ac-electric fields. The dielectric storage $\varepsilon'(\omega)$ and the loss $\varepsilon''(\omega)$ of a multiwalled CNT (MWCNT) sample are reported as a function of amplitude of both $E_{rot}(\omega)$ and $E_{ac}(\omega'=203$ kHz) over the frequency range of $1\leq\omega\leq10^5$ Hz. The results demonstrate how E_{ac} and E_{rot} polarize the curved graphene layers in the MWCNT sample. The dielectric spectra reveal two relaxation modes: a slow mode below 100 Hz that is likely attributed to space-charge polarization at the electrode-nanotube interface and a fast mode in the kilohertz range that is discussed in terms of reorientation polarization of permanent and/or induced electric dipoles.

Following this introduction, a description of the ac-capacitive bridge technique, materials, and sample preparation are given in Sec. II. Dielectric spectra results as a function of applied ac-electric field amplitude are presented in Sec. III, followed by discussions and conclusions in Sec. IV, where a simple physical model is introduced to interpret the fast relaxation mode.

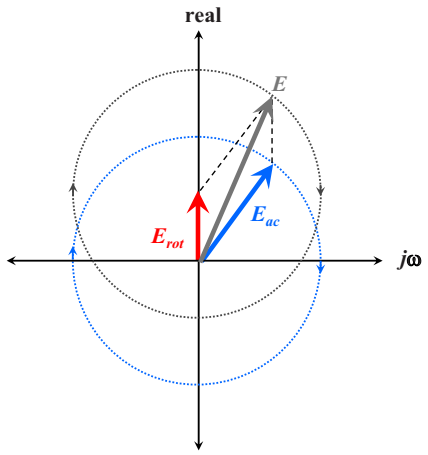

FIG. 1. (Color online) The ac-electric fields E_{rot} and E_{ac} in the *complex rotating frame* of the dielectric measurement. The field E_{rot}, along the real axis, is in phase and at the same frequency as the measurement, hence static in complex rotating frame. Being at a different frequency than the measurement, E_{ac} acts as an ac field in the complex rotating frame. The field E is the resultant field and, at any time, the sample experiences the real component.

a)Electronic mail: gsiannac@wpi.edu.

II. EXPERIMENTAL PROCEDURES

A. ac-capacitance bridge technique

A homebuilt ac-capacitance bridge technique,[22–24] operating with a probing field $E_{\mathrm{rot}}(\omega)$, is used to measure $\varepsilon'(\omega)$ and $\varepsilon''(\omega)$ as a function of frequency and magnitude of E_{rot} and E_{ac}. The capacitive cell consists of a parallel-plate configuration, 1 cm across with a 100 μm gap using a Kapton spacer, housed in a temperature controlled bath. The real and imaginary parts of the complex dielectric constant are determined from the in-phase and $(\pi/2)$ out-of-phase off-balance signals of the bridge. Comparison between the empty capacitor and sample filled capacitor allows for an absolute measurement of $\varepsilon^*(\omega, E_{\mathrm{rot}}, E_{\mathrm{ac}})$. The probing ac-field $E_{\mathrm{rot}}(\omega)$ is applied across the sample through the capacitive bridge and is adjusted by increasing the probing voltage. Because of this technique, the actual magnitude of E_{rot} across the sample is not known (only the driving voltage across the bridge was controlled). However, the factor that E_{rot} increases is known if measured in units of that produced by the lowest voltage (denoted as E_{rot}^0 for a 1 V amplitude applied probing voltage), this factor is labeled $\boldsymbol{e}_R = E_{\mathrm{rot}}/E_{\mathrm{rot}}^0$. To apply and vary the $E_{\mathrm{ac}}(\omega')$ field, a second signal generator, independent of the capacitance bridge, is applied directly across the parallel capacitor plates parallel to the bridge. The presence of E_{ac} can be visualized as making the measurement of $\varepsilon^*(\omega)$ constant in the presence of an ac bias field that is independent of the measurement technique. The frequency of E_{ac} is a constant 203 kHz that is well above the maximum frequency range (100 kHz) of the lock-in amplifier used to detect the off-balance signal and so avoids interference. For consistency, the magnitude of E_{ac} is also labeled $\boldsymbol{e}_{\mathrm{ac}} = E_{\mathrm{ac}}/E_{\mathrm{ac}}^0$, where E_{ac}^0 is that produced using 1 V amplitude output. The quantities $\boldsymbol{e}_R$ and $\boldsymbol{e}_{\mathrm{ac}}$ are the factors that the actual electric field magnitudes increase from their lowest to higher values.

B. Materials and sample preparation

The MWCNT sample, received from Sinha, was used without further processing other than drying under vacuum prior to loading into the spectrometer. The MWCNT sample used is polydisperse containing nanotubes 10–100 nm in diameter and 1–5 μm in length. Approximately 80 vol % of the capacitive cell was occupied by the MWCNT. The sample was filled into the capacitive cell by drop-cast evaporation; thus the orientation of the nanotubes is random between the plates. The measurements reported here are of the *average* complex dielectric constant $\varepsilon^*(\omega) = (\varepsilon_{\parallel} + 2\varepsilon_{\perp})/3$, where $\varepsilon_{\parallel}$ and $\varepsilon_{\perp}$ are the complex dielectric constants parallel and perpendicular to the nanotube long axis, respectively.

III. RESULTS

The dielectric spectra of the MWCNT sample exhibit two well-distinguished dynamic modes in the frequency range studied, as shown in Fig. 2. The slow mode occurring between 20 and 100 Hz is likely due to space charge polarization at the electrode-nanotube interface (denoted mode 1), and the faster mode occurring between 1.5 and 12 kHz is likely due to orientational polarization of permanent and/or induced dipoles (denoted mode 2) either of the nanotubes themselves or within the multiple graphene layers. Mode 1 is strongly coupled to E_{rot}, while mode 2 is independent of E_{rot} (see Fig. 2). The spectra reveal the opposite behavior with the application of E_{ac}. Here, the relaxation frequency increases while the strength (peak height of ε'' for mode 2, $\Delta\varepsilon_2''$) decreases for mode 2 as E_{ac} increases, while mode 1 is independent of E_{ac}.

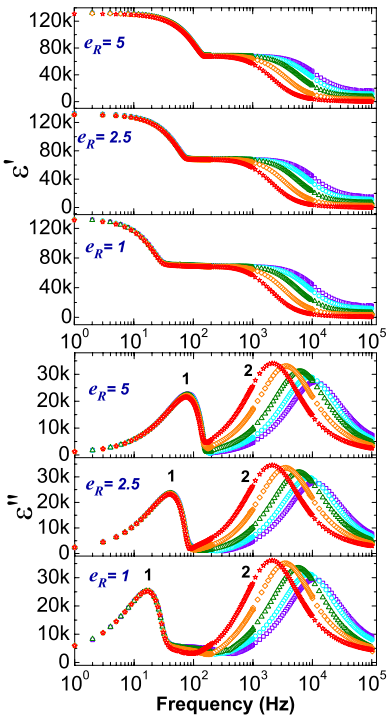

FIG. 2. (Color online) The frequency and E_{ac} (shown by field factor $\boldsymbol{e}_{\mathrm{ac}}$: star=1, diamond=2, triangle=3, circle=4, and square=5) dependence of dielectric storage ε' (top panel) and loss ε'' (bottom panel) of MWCNT sample for three values of E_{rot} (or $\boldsymbol{e}_R$).

Since mode 1 is likely to originate from space charge polarization, it may involve several mechanisms of space charge accumulation at the electrode-nanotube interface. However, all such processes for powder dielectric samples generally occur at low frequency, typically below 100 Hz,[25] and depend strongly on the surface conductivity of the sample and the cell.[21] Note that the probing field E_{rot} is static in the rotating frame and so represents an effective dc field that couples strongly to charge conduction. This should cause the relaxation frequency of mode 1 to shift as a function of $\boldsymbol{e}_R$ but is independent of $\boldsymbol{e}_{\mathrm{ac}}$, as observed in Fig. 2. Figure 3(a) shows the relaxation frequency of mode 1 (f_1) increasing linearly for $0 \leq \boldsymbol{e}_R < 3$. For $\boldsymbol{e}_R > 3$, f_1 appears to begin saturating, reaching approximately $f_1^{\max} \sim 75$ Hz for $\boldsymbol{e}_R > 5$. The observed behavior of f_1 is consistent with conduction of finite space charges built up at the electrode-nanotube (and perhaps nanotube-nanotube) interfaces. To strengthen this interpretation, f_1 extrapolates to zero as $\boldsymbol{e}_R = 0$, further indicating that mode 1 is associated with a charge conduction mechanism that vanishes as the field strength goes to zero.

It is expected that the magnitude of the probing field in an ac-capacitance bridge method (E_{rot}) should not affect the orientational relaxation of permanent or induced

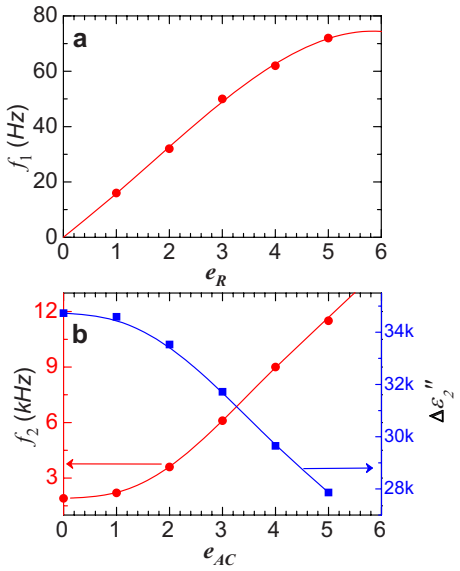

FIG. 3. (Color online) (a) Relaxation frequency of mode 1 (f_1) as a function of $E_{\rm rot}$ (or e_R). Note the initial linear dependence with zero intercept and the apparent saturation for $e_R > 5$. (b) Relaxation frequency of mode 2 (f_2) and dispersion strength ($\Delta\varepsilon''_2$, peak magnitude of ε'') of mode 2 as a function of $E_{\rm ac}$ (or $e_{\rm ac}$) for $e_R = 1$.

dipoles.[22,26–28] Thus, it is expected that the faster mode 2, being associated with a dipole relaxation process, should be independent of $E_{\rm rot}$, as seen in Fig. 2 for constant $e_{\rm ac}$. Figure 3(b) reveals that above a threshold ($e_{\rm ac} \approx 1$ where both $E_{\rm rot}$ and $E_{\rm ac}$ are approximately of equal magnitude), f_2 increases linearly while the strength $\Delta\varepsilon''_2$ decreases linearly with increasing $E_{\rm ac}$.

IV. DISCUSSIONS AND CONCLUSIONS

The observed behavior of mode 2 with respect to $E_{\rm ac}$ may be interpreted by the following simple model, which suggests a unique relaxation mechanism. The multiple graphene layers of a MWCNT can be visualized as an effective capacitor (C) between the layers in series with an effective resistor (R) of the carbon wall. The applied field $E_{\rm ac}$ generates a voltage difference $V = E_{\rm ac} d$ between successive graphene layers in an MWCNT, where d is the average distance between graphene layers. The natural frequency of a single layer element of this analogous RC circuit is given by $\omega_0 = 2\pi f_2 = 1/RC$. The equivalent effective capacitor C for multiple graphene walls is approximately given by $C = (V/Q + V/Q + \cdots n\text{th layer})^{-1} = Q/(nV)$, where n is the number of walls and Q is the charge on the each curved graphene layer. Substituting gives $\omega_0 = Vn/RQ = E_{\rm ac}(dn/RQ)$, a linear dependence of ω_0 with increasing $E_{\rm ac}$ (once $E_{\rm ac}$ is sufficiently above the effect of $E_{\rm rot}$) with all other factors being constant for a given sample. This simple model appears to describe well the observed amplitude dependence of the relaxation frequency of mode 2.

To further illuminate the observed dielectric spectra, an ac-conductivity analysis was conducted. The ac conductivity is related to the dielectric properties by $\sigma_{\rm ac} = \omega\varepsilon''\varepsilon_0$ (Ref. 29) and represents the sum contributions from all dissipative mechanisms. Figure 4 shows the MWCNT sample ac-conductivity frequency dependence and reveals the two

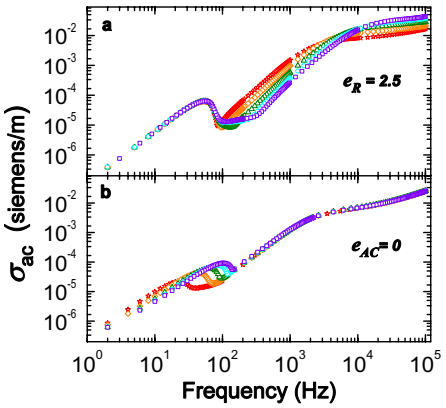

FIG. 4. (Color online) The dielectric ac conductivity $\sigma_{\rm ac}$ of MWCNT sample as a function of frequency. (a) For constant e_R and varying $e_{\rm ac}$: star=1, diamond=2, triangle=3, circle=4, and square=5. (b) For constant $e_{\rm ac}$ and varying e_R: star=1, diamond=2, triangle=3, circle=4, and square=5.

modes seen in the original dielectric spectra. The slow and fast modes are observed with a $\sigma_{\rm ac}(\omega)$ for mode 1 typical of charge conduction, while that for mode 2 reminiscent of that for induced polarization (perhaps, as discussed above, related to that between the graphene layers within a nanotube). For frequencies at or above 50 kHz, $\sigma_{\rm ac}$ exhibits a slow increase above the plateau associated with mode 2, which may be a signature of the mode observed by Ahmad *et al.*[12] at $\sim 10^7$ Hz for the highest volume concentration of MWCNT in alumina.

Finally, a Debye relaxation analysis has been performed on the observed dielectric spectra. A Debye relaxation can be expressed as

$$\varepsilon^* = \left(\varepsilon_\infty + \frac{\Delta\varepsilon}{1+(\omega\tau)^2}\right) - i\left(\frac{\Delta\varepsilon\omega\tau}{1+(\omega\tau)^2}\right),$$

where τ is the relaxation time constant and $\Delta\varepsilon = \varepsilon_0 - \varepsilon_\infty$ is the dielectric relaxation strength (the difference between the static and infinite frequency dielectric constants) for a single relaxation process. Figure 5 shows such a fit and indicates that mode 2 is quite consistent with this form without any additional fitting factor. This confirms that mode 2 is related to a polarization process where charge migration does not

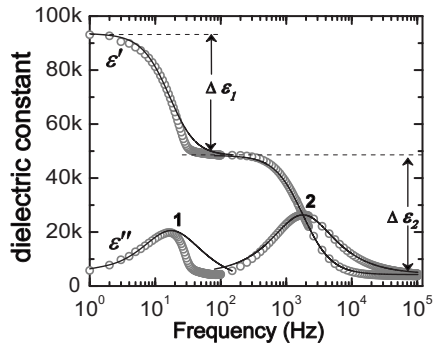

FIG. 5. The dielectric spectrum of the MWCNT sample for $e_R = 1$ and $e_{\rm ac} = 0$; open circles are the data and the solid lines are fits to a Debye relaxation form. Modes 1 and 2 are labeled in the figure, where $\Delta\varepsilon_1$ and $\Delta\varepsilon_2$ are the real dielectric strengths, respectively.

play an important role. Clearly, mode 1 is asymmetric and not a Debye relaxation.

In summary, these results clearly reveal that this nanoscale system can be perturbed by applying ac-electric fields in two different ways: E_{rot} and E_{ac}. The observed electric field dependence of the spectra reveals the polarization mechanism within the graphene layers of MWCNT. A simple theoretical model can explain the observed frequency shift of mode 2 with E_{ac}: capacitor-resistor-like structure of the multiple graphene walls. This model accounts for the coupling of the polarization between multiple graphene layers in MWCNT. The extracted dielectric ac conductivity increases by four orders of magnitude for increasing frequencies up to 100 kHz and suggests a way to tune the suitable value of conductivity of a MWCNT for a given application.

[1]S. Iijima, Nature (London) **354**, 56 (1991).
[2]P. Poncharal, Z. L. Wang, D. Ugarate, and W. A. de Heer, Science **283**, 1513 (1999).
[3]L. Wang and Z.-M. Dang, Appl. Phys. Lett. **87**, 042903 (2005).
[4]Y. Xu, Y. Zhang, and E. Suhir, J. Appl. Phys. **100**, 074302 (2006).
[5]G. L. Zhao, D. Bagayoko, and L. Yang, J. Appl. Phys. **99**, 114311 (2006).
[6]S. Sinha, S. Barjami, G. Iannacchione, A. Schwab, and G. Muench, J. Nanopart. Res. **7**, 651 (2005).
[7]X. Guo, D. Yu, Y. Gaol, Q. Li, W. Wan, and Z. Gao, *Proceedings of the First IEEE International Conference on Nano/Micro Engineered and Molecular Systems*, Zhuhai, China (IEEE, New York, 2006).
[8]O. Stephan, D. Taverna, M. Kociak, K. Suenaga, L. Henrard, and C. Colliex, Phys. Rev. B **66**, 155422 (2002).
[9]A. Madarhri, G. Pecastings, F. Carmona, and M. E. Achour, Journal of Microwaves and Optoelectronics **6**, 36 (2007).
[10]Y. Sato, M. Terauchi, Y. Saito, and R. Saito, J. Electron Microsc. **55**, 137 (2006).
[11]P. Pötschke, S. M. Dudkin, and I. Alig, Polymer **44**, 5023 (2003).
[12]K. Ahmad, W. Pan, and S.-L. Shi, Appl. Phys. Lett. **89**, 133122 (2006).
[13]E. T. Thostenson, Z. Ren, and T.-W. Chou, Compos. Sci. Technol. **61**, 1899 (2001).
[14]R. H. Baughman, A. A. Zakhidov, and W. A. de Heer, Science **297**, 787 (2002).
[15]P. G. Collins and P. Avouris, Sci. Am. **283**, 38 (2000).
[16]A. Javey, Q. Wang, A. Urai, Y. Li, and H. Dai, Nano Lett. **2**, 929 (2002).
[17]R. Martel, T. Schmidt, H. R. Shea, T. Hertel, and P. Avouris, Appl. Phys. Lett. **73**, 2447 (1998).
[18]M. D. Lynch and D. L. Patrick, Nano Lett. **2**, 1197 (2002).
[19]I. Dierking, G. Scalia, and P. Morales, J. Appl. Phys. **97**, 044309 (2005).
[20]S. J. Jeong, K. A. Park, S. H. Jeong, H. J. Jeong, K. H. An, C. W. Nah, D. Pribat, S. H. Lee, and Y. H. Lee, Sr., Nano Lett. **7**, 2178 (2007).
[21]R. Basu and G. Iannacchione, Appl. Phys. Lett. **92**, 052906 (2008).
[22]S. Pilla, J. A. Hamida, and N. S. Sullivan, Rev. Sci. Instrum. **70**, 4055 (1999).
[23]S. C. Bera and S. Chattopadhyay, Measurement **33**, 3 (2003).
[24]M. C. Foote and A. C. Anderson, Rev. Sci. Instrum. **58**, 130 (1987).
[25]G. G. Raju, *Dielectrics in Electric Fields* (Dekker, New York, 2003).
[26]*Relaxation Phenomena*, edited by W. Haase and S. Wrobel (Springer, New York, 2003).
[27]F. Kremer and A. Schonhals, *Broadband Dielectric Spectroscopy* (Springer, New York, 2003).
[28]N. E. Hill, W. E. Vaughan, A. H. Price, and M. Davies, *Dielectric Properties and Molecular Behavior* (Van Nostrand Reinhold Co., London, 1969).
[29]*Dielectric Materials and Applications*, edited by A. R. Von Hippel (Chapman and Hall, London, 1954).